DOI: 10.21062/mft.2023.084 © 2023 Manufacturing Technology. All rights reserved. http://www.journalmt.com

An Investigation into Conventional Spinning Process Using Ball Shaped Rollers as Forming Tool

Ayman Ali Abd-Eltwab (0000-0003-0384-771X)[1]*, Gamal I. Helal (0009-0008-6346-1556)[2], Mohamed N. El-Sheikh (0000-0002-9571-7594)[2], Essam Khalaf Saied (0000-0002-6708-9287)[1], Ahmed M. Atia (0000-0003-1179-382X)[3]
[1]Mechanical Engineering Department, Faculty of Engineering, Beni-Suef University, Beni-Suef 62511, Egypt.
[2]Mechanical Department, Faculty of Technology and Education, Beni-Suef University, Beni-Suef 62511, Egypt.
[3]Mechanical Design and Production Engineering Department, Faculty of Engineering, Assiut University, Assiut, Egypt.
* Corresponding author Phone: +20-01005728351, Mail: AymanAli@eng.bsu.edu.eg

Conventional spinning is one of the oldest processes used widely in manufacturing to obtain cup shape products. Conventional spinning is the technique that produces axisymmetric part or component over rotating mandrel with the help of rigid tool known as rollers. The shape of roller is a very important parameter for the success of the spinning process. The present research is aiming to use ball shaped rollers as forming tools in conventional spinning process experimentally. The experimental work was carried out on the center lathe machine as forming machine, the spinning tool or spinning rollers were installed on a dynamometer replaced the tool post while the mandrel was mounted on the lathe chuck. The spinning tool in this work consists of three rollers performing conventional spinning. The set of rollers is mounted on jaws of lathe chuck which working as a holder for the spinning tool parts. The experimental work was conducted in order to test the proposed tool and investigate the influence of the main conventional spinning parameters (mandrel rotational speed, axial feed and blank diameter or spinning ratio) on the process forming load and the product quality. The response of the product quality and required load to process parameters such as rotational speed (76,150, 230 and 305 rpm), axial feed (0.08, 0.15,0.3, and 0.6 mm/rev) also examined new rollers in different mandrel diameters 45, 60 and 80 mm. The experimental results showed that, the suggested tool acquired a spinning ratio of 2.17 which is about 35% greater than the announced conventional spinning ratio of 1.6 without any addition to the tool just using the suggested Ball shaped roller arrangement. The mandrel rotational speed, and axial feed rate are the most pronounced parameters, which have great effects on the forming loads during the spinning process.

Keywords: Conventional spinning, Ball shaped rollers, Spinning tool, Mathematical model, Forming load, Spinning ratio

1 Introduction

Metal forming is a competitive manufacturing technique that may generate a variety of items with diverse forms and sizes. Metal forming is a manufacturing process that utilizes forces to deform metal plastically into a desired shape. It is a flexible process that can be used to produce a wide variety of parts, from simple shapes to complex assemblies. Metal forming is important for several reasons, including its cost-effectiveness, enhanced mechanical properties, flexibility, higher productivity, and considerable material saving [1-3]. Furthermore, it is a widely used process in a variety of industries, including automotive, aerospace, and manufacturing [4, 5].

Sheet metal forming can produce parts with very good dimensional accuracy. The deformation process in sheet metal forming is controlled by the tooling, so the parts are more likely to have the desired dimensions. Otherwise, in the machining process the accuracy of the parts is more dependent on the skill of the machinist one way or another [5, 6].This has been obvious in the domains of mechanical engineering in recent years, as has the need for study in the field of metal forming. The following is a review of some significant research in this topic.

Eamonn Quigley and et al .[7], have proposed different analyses of the metal spinning process. These highlight common process limitations. An analysis of the process is presented which shows how the strains involved are quite different resulting in different spinning techniques. Results are interpreted to explain the rationale for multi-pass spinning operations.

Omolayo M. Ikumapayi and et al.[1], investigated the bending operation in sheet metal forming. There are different types of bending techniques that were

exploited and presented at varying Moden time in manufacturing process. In addition, the theory of bending was also discussed extensively in this paper. Results reveal that for conventional spinning the strains involved are much less than for shear forming.

E M Mamros et al, [2] discusses the use of tool rotation in the flaring process of thin-walled tubes. The study found that the rotational speed of the tool can influence the ability of the tube to flare, and that the expansion ratio can be maximized with a decreased amount of friction, a lower rotational speed of the flaring tool, and with an increase in tool velocity. The researcher also performed an analysis of the expansion ratio, strain path, and failure limit of the flaring process. They found that the expansion ratio is influenced by the frictional effects between the tool and the tube, as well as the strain path of the material. The failure limit of the flaring process was found to be dependent on the material properties of the tube and the tool geometry.

Marko Knezevic et al [8] , describes the main results from an experimental investigation into the consequence of cyclic bending under tension on elongation-to-fracture and strength of AZ31 sheets. The authors conclude that the microstructural features have only a secondary effect on the strength behavior of the alloy. The observed behavior is attributed to the formation of cellular substructures during the processing. Significantly, it is shown that the strength of the alloy can be increased by over 30% while preserving at least 5% of its ductility.

Shiori Gondo et al, [9] represent a study of the evolution of the texture distribution during spinning can be evaluated by calculating the crystal orientation density indicated by the small Miller indices. The difference in texture distribution can be systematically compared using cosine similarity and Euclidean distance. In addition, shear spinning was similar to that of the wall part for conventional spinning. In particular, the distribution near the mandrel corner part for conventional spinning resembled that for under-spinning, whereas the distribution in the wall part resembled that for overspinning.

P.F. Gao et al, [10] developed a model to predict the deformation mode and wall thickness variation in the conventional spinning of 1060 aluminum alloy. The model considers the effects of processing parameters and the actual variation in wall thickness. The model was shown to be more exact than the traditional wrinkling model, and it can be used to improve processing design and forming accuracy. So, the results of this study increase the understanding of deformation behavior in conventional spinning. They found that there are three deformation modes shear deformation, compression-shear deformation, and tension-shear deformation. These modes correspond to the wall thickness variation of sine-law reduction, a reduction intermediate between sine-law reduction and no reduction, and wall thickening.

Riaz, A. A. et al, [11] proposed a research investigated the effects of rotational speed on the forming temperature and microstructure of AA-2219-O and AA-2219-T6 sheets during incremental sheet metal forming (ISF). The results showed that the T6 sheet had a higher temperature rise rate than the annealed sheet, due to its higher friction coefficient. This resulted in the T6 sheet failing to achieve the desired forming depth of 25 mm when the rotational speed exceeded 2000 rpm. The SEM results showed that the density of second phase particles decreased with increasing rotational speed, due to the corresponding temperature rise. However, the particle size in both tempers of AA2219 showed only a slight change with increasing rotational speed. In general, the results showed that the rotational speed has a significant effect on the forming temperature and microstructure of AA-2219 sheets during ISF.

Li Zixuan et al [12], simulated five different roller trace curves using a multi-pass conventional spinning simulation model. They also conducted experiments using superalloy GH3030 to verify the results of the simulation. The results of the study showed that the curve trace parameters play a key role in the product thickness uniformity. The distribution of Bezier and conchoid roller traces was more uniform than the other traces. The axial force of the mandrel is also an important factor in the design of tool load capability. Larger roller feed ratio and proper roller traces can reduce the thinning which may avoid the cracks.

To ensure a final product of high precision and accuracy[13], the manufacturing process requires following a precise and meticulous production process. Numerical simulation of production processes is becoming increasingly important and becoming an essential part of the pre-production phase of sheet metal forming processes[14] . Thin sheets of aluminum alloys are widely utilized in various industries[15]. The production of gas cylinders by spinning essentially eliminates the defects related to welding in the traditional production process[16].

In conclusion, metal forming is an adaptable and significant process that is used to produce a wide variety of parts for a variety of industries. It is a cost-effective, flexible, and productive process that can help to improve the mechanical properties of metal parts. Therefore, from the aforementioned, the authors of this article presented their studies in the field of sheet formatting.

2 Mathematical and geometrical analyses

The main object of this theoretical analysis is to guess the amount of load needed to complete the

process of conventional spinning. This is mainly to decide which machine we can use in conventional spinning.

2.1 Analytical Model Analysis

The process can be described as follows to conduct the analysis in order to calculate the maximum load needed for the process. The rollers are moving axially toward the blank which is rotating. This causes the rollers to convert the blank to cup. The forming load required is figured out by the blank reaction on the rollers. The model works for various parameters such as rollers diameter, blank diameter, feed rate, and blank material specifications. The contact area generated between the rollers and blank material has a great effect on the spinning loads in the three directions. An analysis of the area is required in order to develop the model. The maximum load areas were defined to obtain the load along the rollers stroke. Figure 1 depicts the mechanisms for three-dimensional forming processes, with the X-direction as the axial, the Y-direction as the radial, and the Z-direction as the tangential axis.

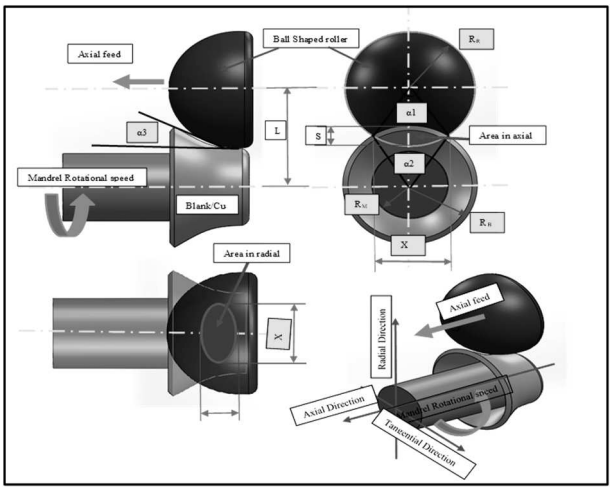

Fig. 1 *The mechanism of spinning process with contact area between roller and blank in three directions*

2.2 The Forming Load

Three elements can be used to break down the total load (FT) needed for the forming process (FX, FY, and FZ components). The calculations were considered on the following hypotheses:

- (i) It is possible to ignore the strain hardening fluctuation throughout the forming process.
- (ii) It is possible to ignore the spring-back effect.
- (iii) The spinning substance possesses homogeneity, isotropy, and incompressibility.
- (iv) During the deformation, the effects of temperature and speed can be ignored.

The axial load (FX), radial load (FY), and tangential load (FZ) are the three load components. This loads' calculation is provided by:

$$F_T = \sqrt{F_X{}^2 + F_Y{}^2 + F_Z{}^2} \quad (1)$$

Utilizing a semi-empirical technique of stress analysis for the initial load component. Under the state of plane strain, the direct yield condition or effect stress $\bar{\sigma}$_maxis given by [13] the maximum axial stresses $\bar{\sigma}$_max in cross sectional area of the ring, AR was;

$$\bar{\sigma}_{max} = K_f \, \varepsilon^{n+1} \quad (2)$$

Where $\bar{\sigma}_{max}$ is the maximum stress and ε the strain can be expressed by following equation.

$$\varepsilon = \ln \frac{R}{r} \quad (3)$$

$$K_f = \frac{K}{1+n} \quad (4)$$

Where:

$$R = \frac{D_B}{2} = R_B \quad (5)$$

$$r = \frac{D_m}{2} + S_o \quad (6)$$

The normal force acting on contact area A is provided by.

$$\mathrm{F} = \bar{\sigma}_{max} * \mathrm{A} \quad (7)$$

Where A is the circular area of the sphere segment. The spinning loads components can be expressed by

$$\mathrm{F_X} = \bar{\sigma}_{max} \mathrm{A_X} \quad (8)$$

$$\mathrm{F_Y} = \bar{\sigma}_{max} \mathrm{A_Y} \quad (9)$$

$$\mathrm{F_Z} = \bar{\sigma}_{max} \mathrm{A_Z} \quad (10)$$

2.3 The Contact Surface Area in three directions

During the process of forming, contact surfaces will appear between the blank material and the rollers. Since these contact surfaces are not constant during the process. It can be described as an area changed from zero to maximum value being constant for a while during the process then decreasing to zero at the end of the process. The point where the ball's circumferential surface intersects with the surface of the blank during the forming process. Analytically speaking, this kind of surface is difficult to characterize [14]. However, the calculation of force components is aided by the determination of its estimated areas. From the geometry of the process the maximum total contact area during one revolution can be obtained as follows.

$$A_X = 3 * \frac{\pi\, D\, S_v}{Cos\ \alpha 3} \tag{11}$$

Where the instantaneous effective contact area in axial direction is given as the ratio between instantaneous contact angle θ and the total angle 360 degrees. Hence, the axial projected area is calculated as follows:

$$A_X = 3 * \frac{\theta}{360} * \frac{\pi\, D\, S_v}{Cos\ \alpha 3} \tag{12}$$

While the instantaneous contact area in radial direction is given as follows:

$$A_Y = (R_R - R_R * \mathrm{Cos}\ \alpha 2)\,(R_B - R_B * \mathrm{Cos}\ \alpha 1) * S_v\, Sin\alpha 3 \tag{13}$$

Also, the elliptic tangential contact area between the 3-rollers and the blank can calculated as follows:

$$A_z = 3\,(A_1 + A_2) = 3\left(\left[\left(\frac{Y_1}{12\,X}\right) 3\,{Y_1}^2 + 16\,X^2\right] + \left[\left(\frac{Y_2}{12\,X}\right) 3\,{Y_2}^2 + 16\,X^2\right]\right) \tag{14}$$

$$Y_1 = R_R\,(1 - \mathrm{Cos}\ \alpha 1)\,, Y_1 = R_B\,(1 - \mathrm{Cos}\ \alpha 2) \tag{15}$$

The instantaneous contact angles θ, α1, α2 and α3 can be derived from Figure 1 as follows:

$$Cos\ \alpha 1 = 1 - \left(\frac{{R_B}^2 - (R_m + S_o)^2}{2 * R_B * L}\right) \tag{16}$$

$$Sin\ \alpha 1 = \sqrt{\left[\left(\frac{{R_B}^2 - (R_m + S_o)^2}{2 * R_B * L}\right)\right]\left[2 - \left(\frac{{R_B}^2 - (R_m + S_o)^2}{2 * R_B * L}\right)\right]} \tag{17}$$

Where L is the distance between the center of forming tool and the center of the blank is explained by:

$$L = \frac{D_m}{2} + R_R + S_o \tag{18}$$

$${R_R}^2 = {R_B}^2 + (R_m + R_R + S_o)^2 - 2\,R_B * (R_R + R_m + S_o) Cos\ \alpha 2 \tag{19}$$

$$Cos\ \alpha 2 = \left(\frac{{R_B}^2 + {R_m}^2 + {S_o}^2 + 2(R_R\,R_m) + 2(R_R\,S_o) + 2(R_m\,S_o) - {R_R}^2}{2 * R_B * (R_R + R_m + S_o)}\right) \tag{20}$$

$$Sin\ \alpha 2 = \sqrt{1 - \left(\frac{{R_B}^2 + {R_m}^2 + {S_o}^2 + 2(R_R\,R_m) + 2(R_R\,S_o) + 2(R_m\,S_o) - {R_R}^2}{2 * R_B * (R_R + R_m + S_o)}\right)} \tag{21}$$

$$\tan \alpha 3 = \frac{X/2}{S_v} \tag{22}$$

Where X, is the distances shown in Figure 1 and it is expressed as:

$$\mathrm{X} = \sqrt{{R_\mathrm{R}}^2 - \left(\frac{{R_\mathrm{R}}^2 + L^2 - {R_m}^2}{2L}\right)^2} \tag{23}$$

By substituting equations 11to 23 in equations 8, 9 and 10.

$$\mathrm{F_X} = \bar{\sigma}_{max} \mathrm{A_X} = \frac{K}{1+n}\left(\ln\left(\frac{R_B}{\frac{D_m}{2} + S_o}\right)\right)^{n+1} * 3 * \frac{\theta}{360} * \frac{\pi\, D\, S_v}{Cos\ \alpha 3} \tag{24}$$

$$\mathrm{F_Y} = \bar{\sigma}_{max}\, \mathrm{A_Y} = \frac{K}{1+n}\left(\ln\left(\frac{R_B}{\frac{D_m}{2} + S_o}\right)\right)^{n+1} * (R_R - R_R * \mathrm{Cos}\ \alpha 2)\,(R_B - R_B * \mathrm{Cos}\ \alpha 1) * S_v\, Sin\alpha 3 \tag{25}$$

$$\mathrm{F_Z} = \bar{\sigma}_{max}\, \mathrm{A_Z} = \frac{K}{1+n}\left(\ln\left(\frac{R_B}{\frac{D_m}{2} + S_o}\right)\right)^{n+1} * 3\,(A_1 + A_2) = 3\left(\left[\left(\frac{Y_1}{12\,X}\right) 3\,{Y_1}^2 + 16\,X^2\right] + \left[\left(\frac{Y_2}{12\,X}\right) 3\,{Y_2}^2 + 16\,X^2\right]\right) \tag{26}$$

3 Experimental Work

3.1 Test Rig and used Devices

The proposed spinning tool is a set of three ball-shaped rollers arranged 120° apart, as shown in Figure 2. The spinning blank is a blank of 1050 commercial aluminum, as received from the local market. The Test Rig as shown in Figure (3) consists of: the ball shaped roller (2) and the lathe chuck (3) which acts as a carrier for the three rollers. The tool group (2and 3) is attached to the dynamometer (4) which is used to measure the process required force in the three dimensions X, Y and Z. the mandrel (5) which is fixed to the lathe machine (1) chuck. The spinning blank (6) is fixed to the mandrel. The dynamometer is connected to the data logger (7) to transfer the acquired force data to the laptop to be saved for future discussion.

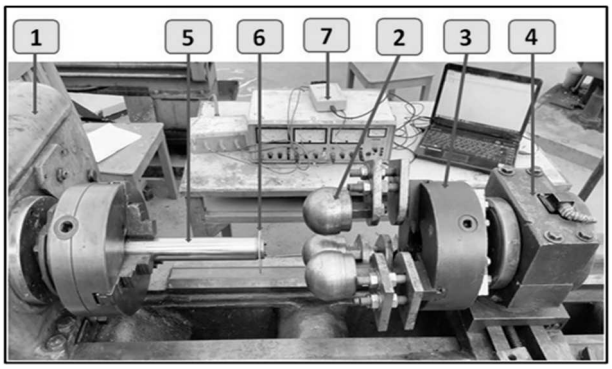

Fig. 2 *Experimental set-up of the conventional spinning process. (1) lath machine (2), (3) forming tool (4) dynamotor (5) mandrel (6) specimens (7) data acquisition system with a computer device*

The blanks were annealed before the experiments to remove residual stresses from material. The annealing process was performed by heating the blanks to a temperature of 450oC for two hours and letting them cool to room temperature inside the furnace. This process takes about 24 hours. The blank thickness was selected to be 3 mm. The blank diameter which also identifies the spinning ratio (ratio of the blank diameter to the mandrel diameter) was selected from 90 to 96 mm with steps 2 mm.

The blank is fixed with the mandrel which was tightened on the lathe chuck to give it the ability of rotation with the chuck. The tool is fastened on the lathe carriage in the place of the lathe tool post to give the tool the ability of automatic feeding toward the blank. The clearance between the mandrel and the rollers was adjusted by moving the jaws toward the mandrel by means of the jaws screw, this clearance is equal to the blank thickness. After the tool was adjusted, the process started with running the lathe to give the mandrel the required rotational speed, the tool takes its feed rate from the movement of the carriage toward the blank. The rollers perform conventional spinning. After performing the process, the tool was retreated to its initial place and the final cup was removed from the mandrel. The complete procedure of the experiments and testing.

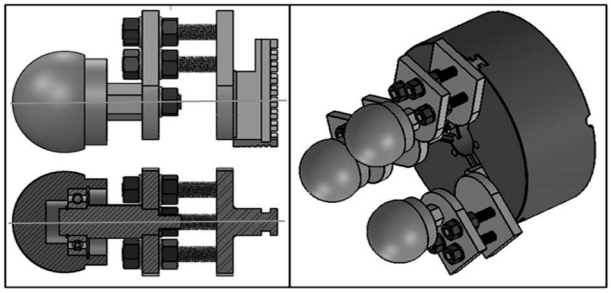

Fig. 3 *Cross section in the conventional spinning tool*

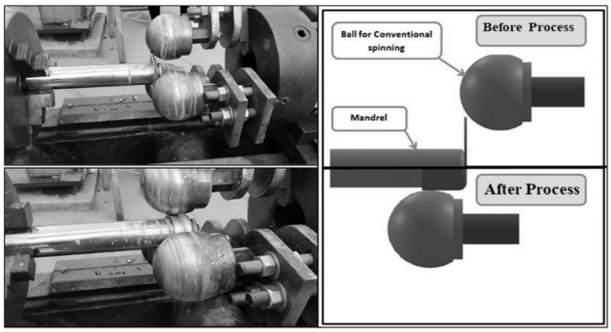

Fig.4 *the conventional spinning process before and during process*

3.2 Measure instruments and Process Variables

The different operating conditions of the forming process for manufacturing cups are depicted in Table 1. The experiments were carried out, and the influence of these parameters on the deformation loads.

Tab. 1 *Parameters of calculation of forming loads components*

No.	Parameter	Symbol	Unit	Value
1	Material of the workpiece			Al.
2	Diameter of the workpiece	do	mm	90- 96 step 2
3	mandrel Rotational speed	N	Rev./min	76, 150, 230 and 305
4	Axial feed	f	mm/rev	0.08, 0.15, 0.3 and 0.6
5	Ball shaped roller diameters	d_b	mm	90
6	Number of forming rollers	N_b		3
7	Mandrel diameters	D_m	mm	45-60-80

4 Results and Discussions

4.1 The Successful produced cups using ball shaped roller

The samples of the cups produced by conventional spinning process with the use of ball shaped rollers are represented in Figures 5 to 11. Figure 5 shows the shape of the aluminium blank before the process of spinning, and next to it is a picture of the cup after it was formed with the spinning tool with ball shaped rollers. Figure 6 is a picture of a group of cups produced according to some variables to show the shape of the produced cup, and it is a sample of good shape and roundness.

Fig. 5 *Blanks with produced cup formed by conventional spinning process*

Fig. 6 *Successful produced cups using ball shaped roller as forming tool in conventional spinning process*

The produced cups do not have any clear defects, cracks, worn out, or cuts. Figure7 shows four pictures of four groups of samples at different mandrel rotational speeds, feed rates, blank diameters. Figure 8 presents the height of the cup with blank diameters from 90 to 98 mm. Figure 10 stands for three cups produced by the same suggested tool with mandrel of diameters 45-, 60-, and 80-mm. Figure 10 shows another group of cups formed with the same suggested tool, but with the addition of ironing process at the same stroke as the thickness of the sample before forming was 3 mm ironed to be 1 mm. This led to a greater wall length from the case of traditional spinning. Figure 11 stands for some failed samples in which cuts occurred during the forming process. Two failure mode occurs due to high spinning ratio that leads to high axial tension or high feed and rotational speed which increases the forming rate that forces the metal to failure.

Fig. 7 *Produced cups at different condition of affected process parameters*

Fig. 8 *Successful cups at blank diameters 90 mm up to 98 mm*

Fig. 9 *Successful cups at same spinning ratio with different mandrel diameters 45, 60 and 80 mm*

Therefore, the two most common failure modes in the spinning process are pinching and tearing. Pinching occurs when the axial tension in the metal is too high, causing the metal to fold over on itself. Tearing occurs when the forming rate is too high, causing the metal to fracture.These failure modes can be caused by a high spinning ratio, which is the ratio

of the workpiece's rotational speed to the feed rate. A high spinning ratio can lead to high axial tension because the metal is being stretched more quickly. It can also lead to a high forming rate because the metal is being moved through the rollers more quickly.The high axial tension and forming rate can force the metal to fracture, either by folding it over on itself or by tearing it [1-3].

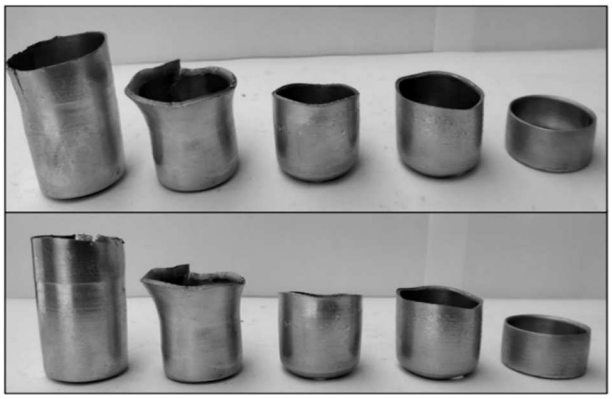

Fig. 10 *Successful cups produced using a forming tool for shear spinning process*

Fig. 11 *Unsuccessful cups at blank diameters upper 98 mm*

4.2 The effect of the axial feed and rotational speed on the forming load

To study the effect of the process variables on the forming load, several mandrel rotational speeds were examined with several feed rates at different blank diameters. Figure 12 presents the relationship of the forming load with the blank diameters at different speeds and feed rates. The forming load is higher at large blank diameter of 96 mm and less than that in the smaller diameters of 90-92-94 mm.

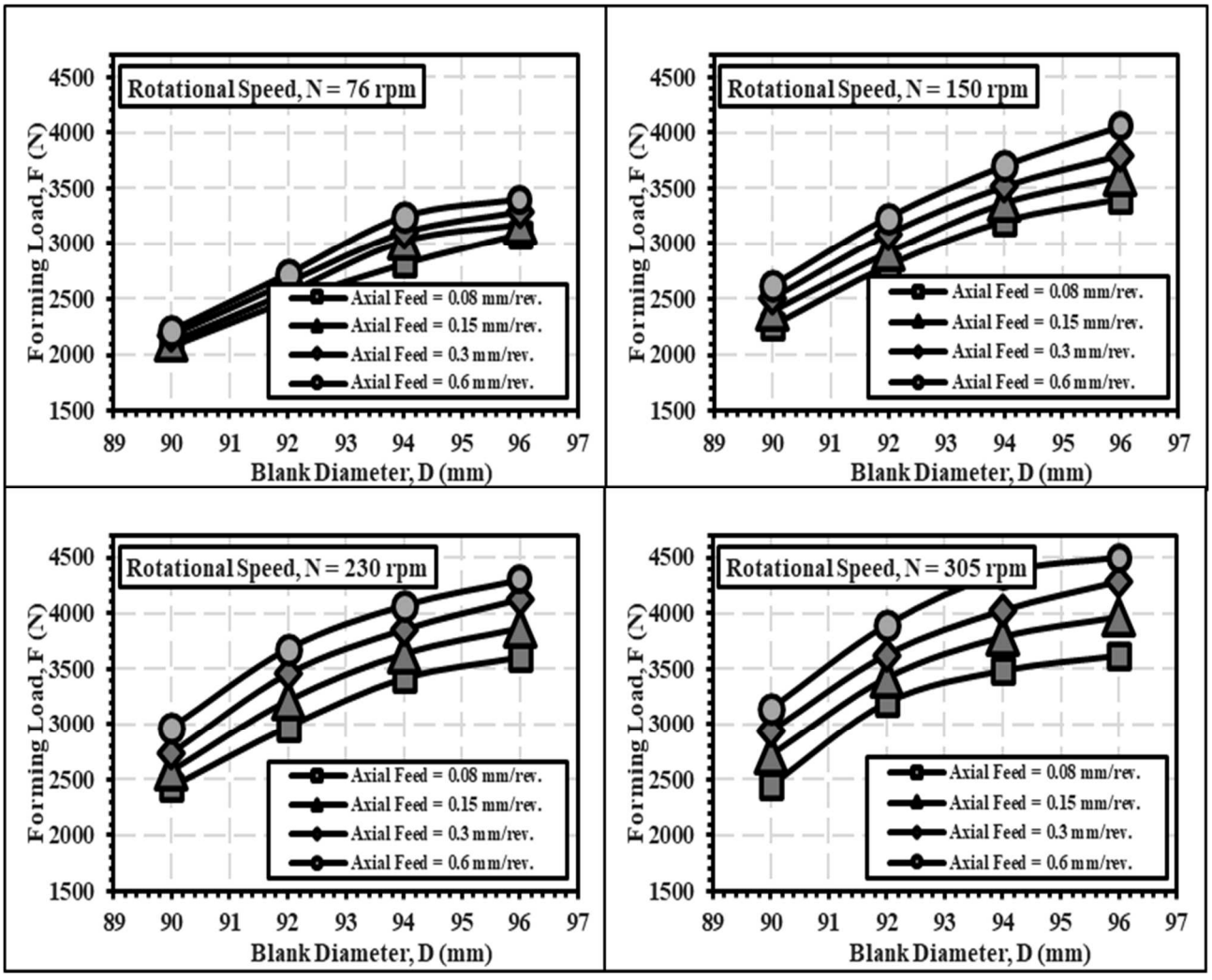

Fig. 12 *Forming load against blank diameters at different axial feeds for rotational speed 76, 150, 230 and 305 rpm*

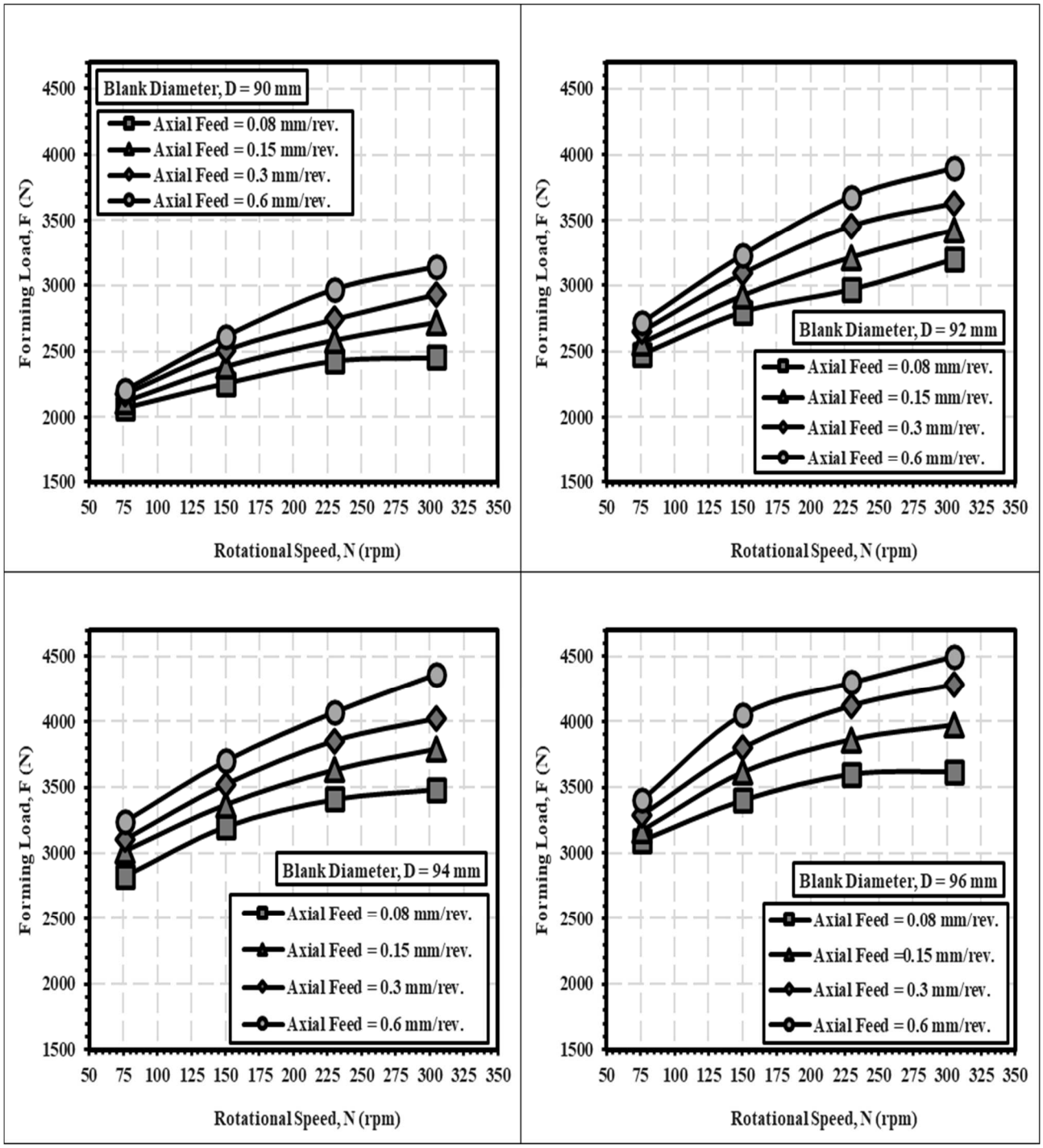

Fig. 13 *The effect of rotational speed on the forming load at different axial feeds for blank diameters 90, 92, 94 and 96 mm*

It is clear that the load increases when using a larger blank diameter as a result of the increase in the drawing ratio and the increase in the amount of metal in front of the forming tool. Figure 13 stands for the relationship of the forming load with the different speeds at different blank diameters and feeds of 0.08-0.15-0.3-0.6 mm/rev. it can be seen that there is an increase in the forming load with the increase of the mandrel rotational speed due to the increase of the forming rate during the process. At smaller speeds, the load values are close, and the divergence of the values increases at high speeds this may be due to the fact that the high speeds with the same feed rates the roller passes many times on the same pass which increases the strain hardening of the blank.

The relationship between the forming load and the feed rate at different speeds and diameters of 90-92-4-96 mm is shown in figures 13 and 14. It is clear that a slight increase in the forming load resulted from changing the feed rate at all speeds and all specified diameters. This increase may be due to the increase in the rate of the amount of displaced metal in front of the roller, which is called the formation rate.

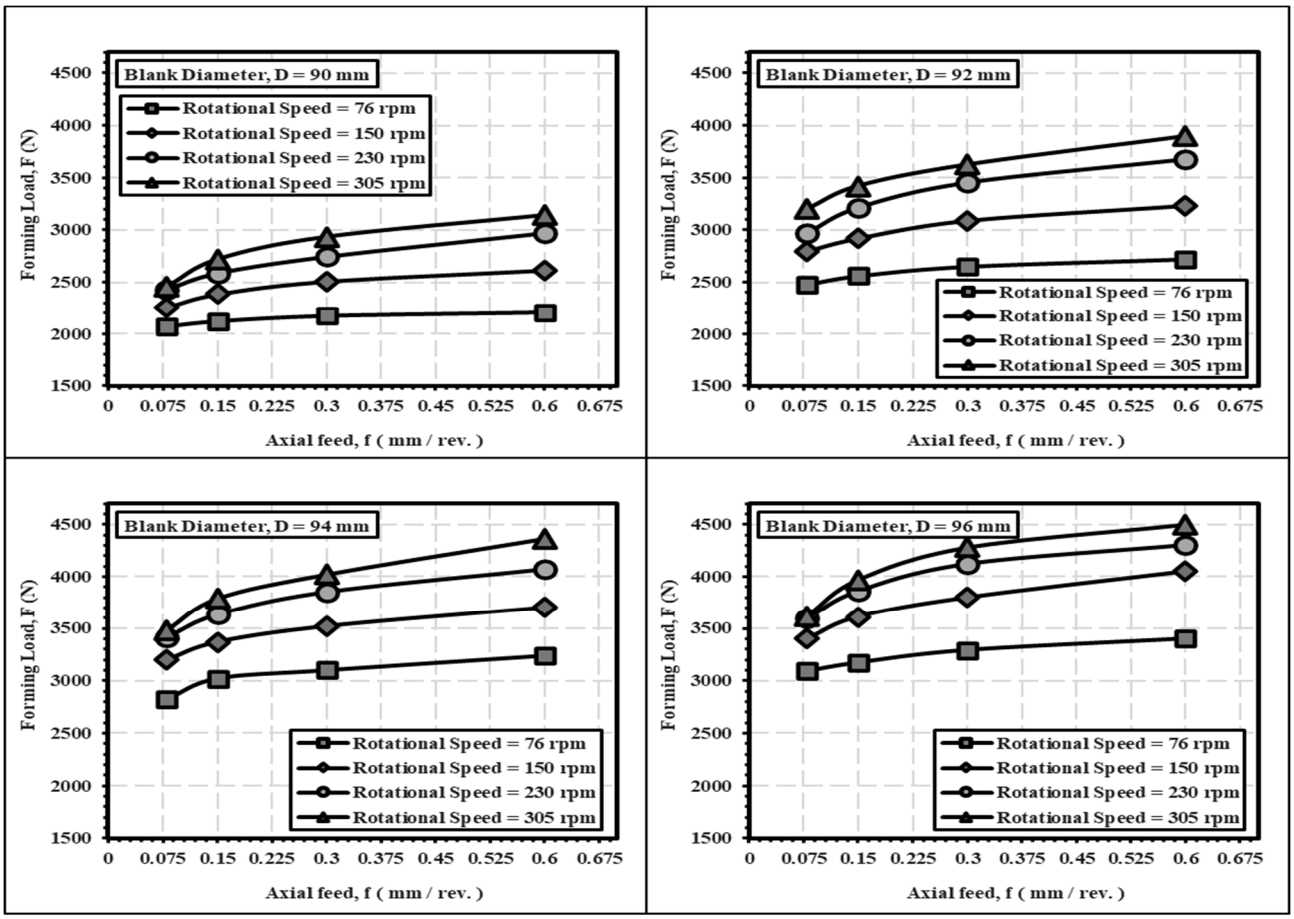

Fig. 14 *The effect of axial feed on the forming load at different rotational speeds for blank diameters 90, 92, 94 and 96 mm*

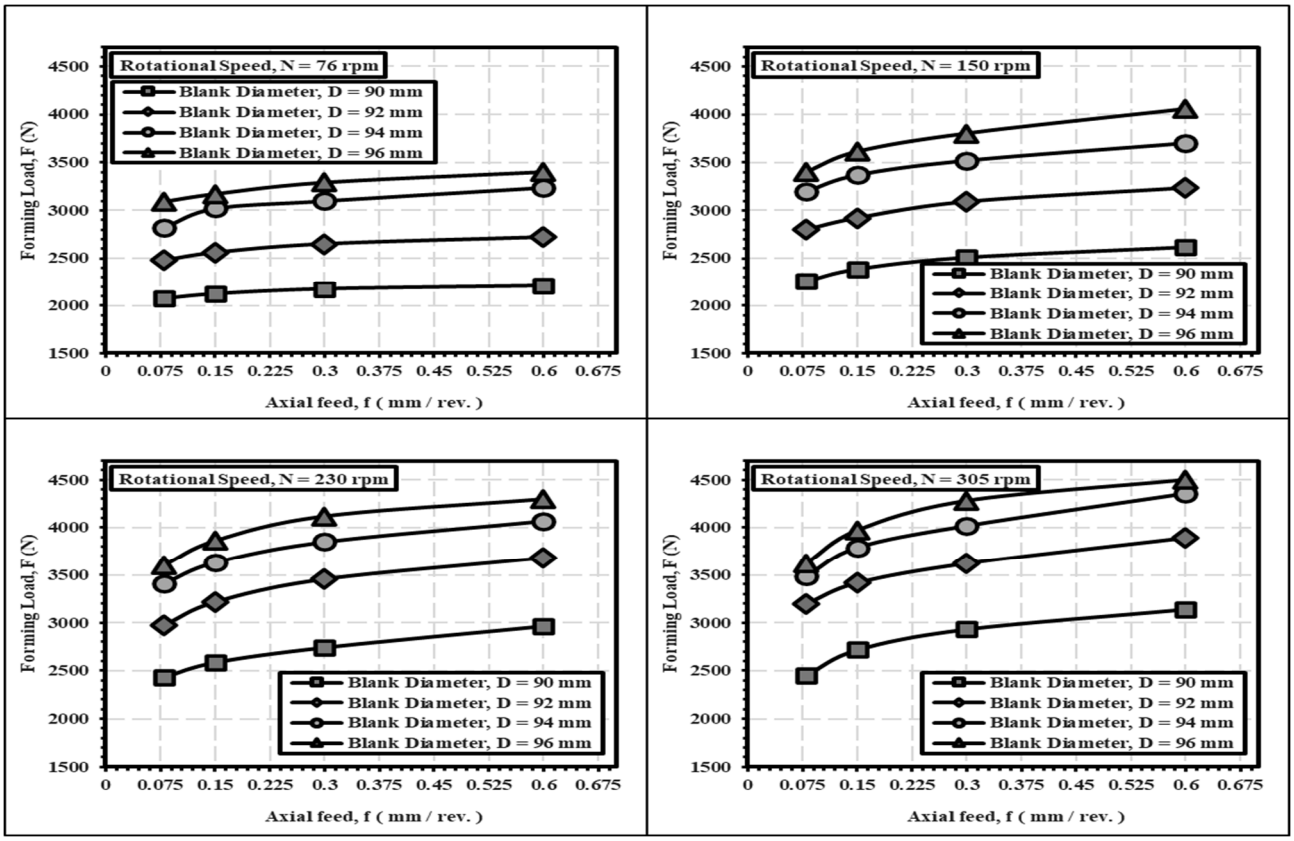

Fig. 15 *Forming load against axial feed at different blank diameters for rotational speed 76, 150, 230 and 305 rpm*

4.3 Effect of axial feed and rotational speed on the produced cups

The thickness variation across the cup wall can be measured by the use of a dial gauge indicator with the aid of a ball against the dial gauge indicator end as shown in figure 16. The ball is used to maintain full contact with the curved inner surface of the specimen. The wall thickness variation of the produced cup must be known to decide the effect of the process parameters on the thickness. Also, the cup application may be affected by the wall thickness variation. As it can be shown in figures 16 to 18 that the thickness variation is about 10% of the original blank thickness which is in most application is an acceptable percentage.

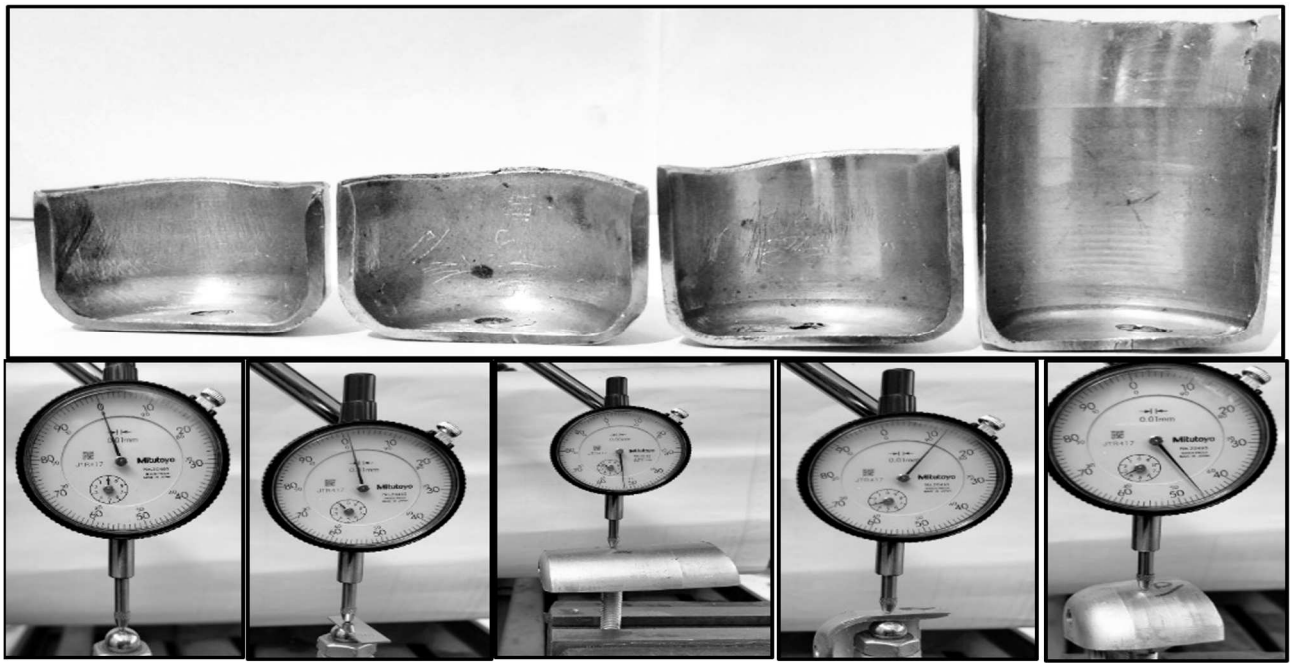

Fig. 16 *Measurement for the wall thickness of cup*

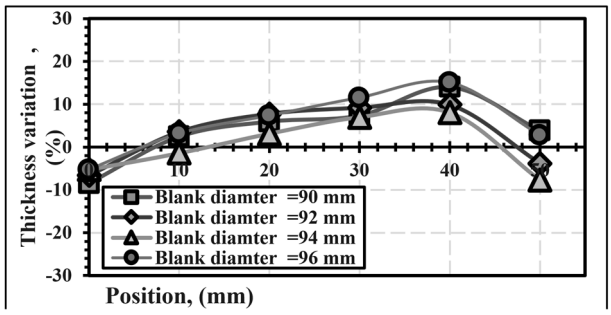

Fig. 17 *Thickness variation against position on wall cup for different blank diameters*

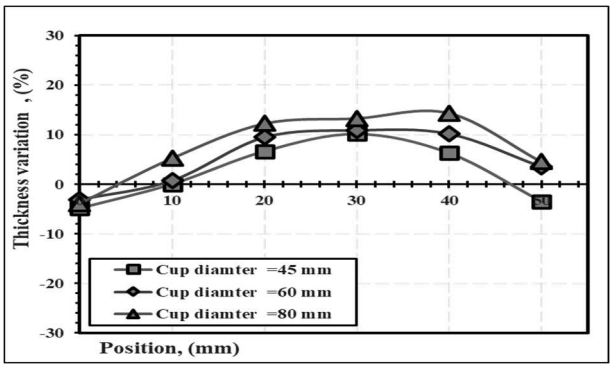

Fig. 18 *Thickness variation against position on wall cup for different cup diameters*

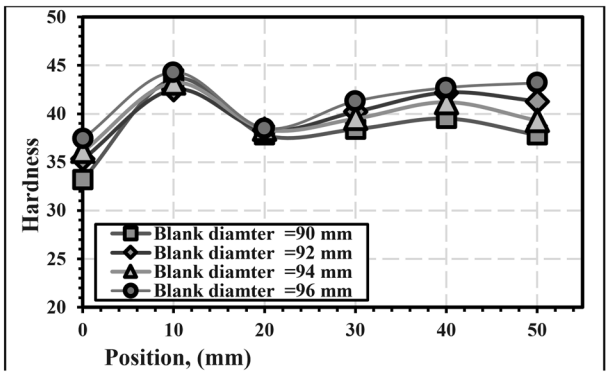

Fig. 19 *Hardness against position on wall cup for different blank diameters*

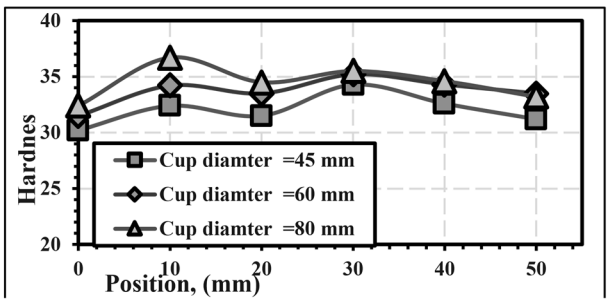

Fig. 20 *Hardness against position on wall cup for different cup diameters*

It can also be controlled using larger blank thickness and conduct corrective ironing process after the conventional spinning process is completed. Some hardness measurements of the produced cups at different cases are shown in figures 19 and 20. The hardness is between 30 and 45 VMH which is an acceptable value of hardness for most applications, especially cooking utensils.

4.4 Comparison of calculated and experimental outcomes

Figures 21 and 22 depict theoretical and experimental results for forming load comparison at axial feeds of 0.08, 0.15, 0.3, and 0.6 mm/rev. It is seen that the load increases with increasing axial feed. Additionally, the load component in direction x-axis is bigger than the other two force components. While the load component in direction z-axis is the smallest. The deviation between the theoretical and experimental results is about 12%.

However, The axis diameter decreases as the axial feed increases. This is because the axial feed stretches the metal, which causes the diameter to decrease.The theoretical axial feed values are shown as dashed lines, and the experimental axial feed values are shown as solid lines. The experimental values are slightly higher than the theoretical values, which is due to the friction between the metal and the rollers.The forming load, F, increases as the axial feed increases. This is because the higher axial feed requires more force to stretch the metal.The graph shows that the axis diameter decreases at a faster rate for higher axial feed values. This is because the higher axial feed stretches the metal more quickly.The forming load also increases at a faster rate for higher axial feed values. This is because the higher axial feed requires more force to stretch the metal more quickly.Overall, the graph shows that the axis diameter decreases and the forming load increases as the axial feed increases. This is due to the fact that the axial feed stretches the metal, which causes the diameter to decrease and the forming load to increase.

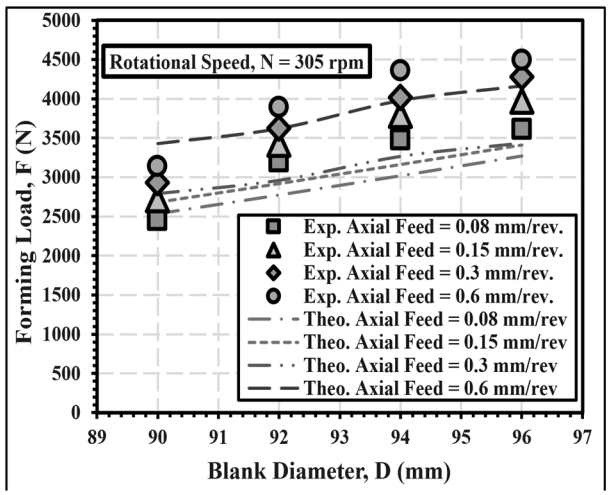

Fig. 21 *Validation theoretical with experimental results at blank diameters*

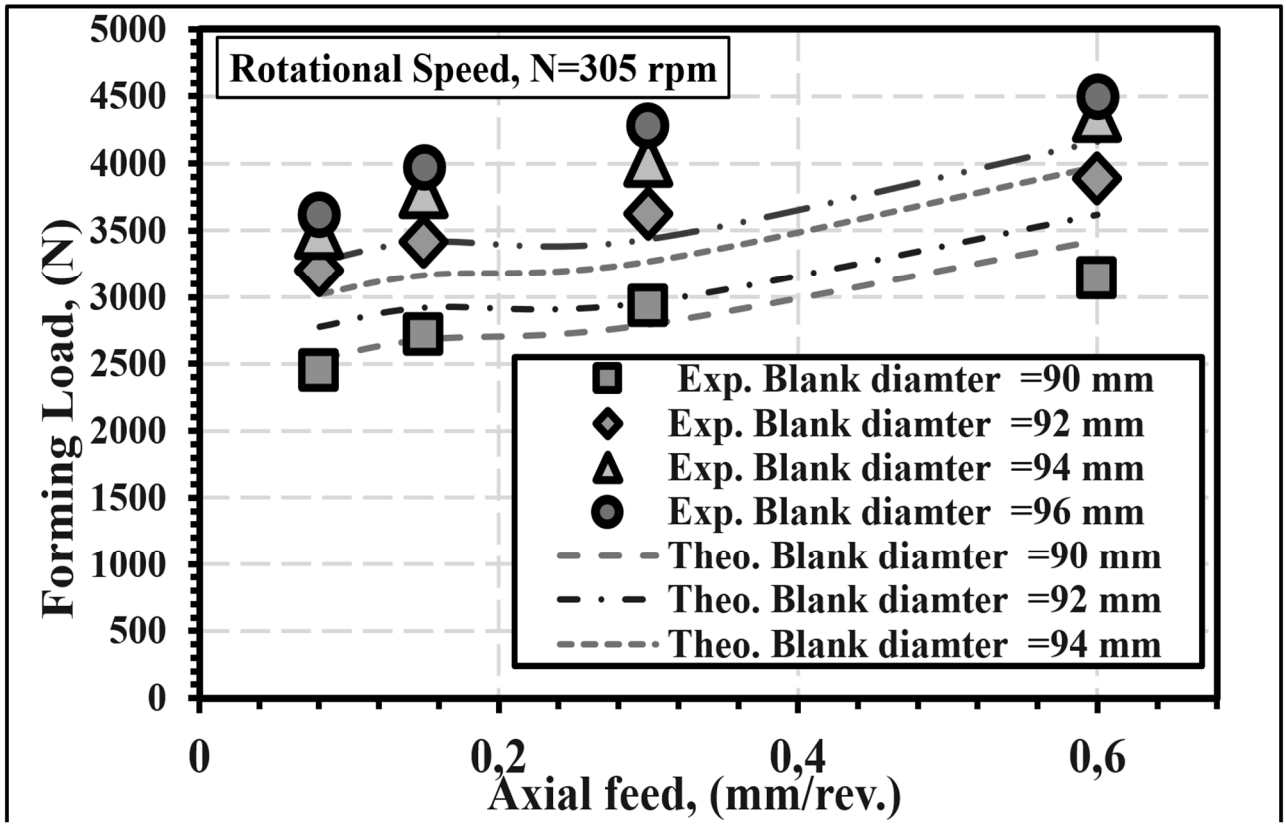

Fig. 22 *Validation theoretical with experimental results at axial feed*

Tab. 2 *Errors between the theoretical and experimental results for forming loads*

Forming loads		Theoretical Force	Experimental Force	Value of Deviation	Deviation %
D_B=90mm	0.08	2538.49	2455	-83.49	-3.40
	0.15	2680.65	2718.5	37.849	1.39
	0.3	2794.90	2933	138.09	4.70
	0.6	3427.43	3140	-287.43	-9.15
D_B=92mm	0.08	2775.96	3200	424.03	13.25
	0.15	2919.13	3420	500.86	14.64
	0.3	2962.50	3624	661.49	18.25
	0.6	3619.76	3895	275.23	7.06
D_B=94mm	0.08	3020.13059	3486	465.86	13.36
	0.15	3163.53346	3790	626.46	16.52
	0.3	3266.929909	4020	753.07	18.73
	0.6	3976.159139	4360	383.84	8.80
D_B=96mm	0.08	3270.523195	3620	349.47	9.65
	0.15	3413.342572	3970	556.65	14.02
	0.3	3434.526972	4280	845.47	19.75
	0.6	4162.553327	4500	337.44	7.49

5 Conclusions

- The new suggested ball shaped tool can achieve a spinning ratio of 2.17.
- Rotational speed and axial feed are affecting the process load and the product quality.
- The forming load increased with the increase of rotational speed, and axial feed**.**
- The conclusions of an analytical model that was generated for predicting forming load were found to be in close agreement with the findings of an experiment.

References

[1] IKUMAPAYI, O.M., et al. A Brief Overview of Bending Operation in Sheet Metal Forming. in *Advances in Manufacturing Engineering*. 2020. Singapore: Springer Singapore.

[2] MAMROS, E. AND C. NIKHARE. Experimental investigation on tube flaring with a rotating tool. in *IOP Conference Series: Materials Science and Engineering*. 2018. IOP Publishing.

[3] HAZAWI, A., R. ABDEL-MAGIED, AND M. ELSHEIKH, an experimental analysis of a flaring process for tube ends using a novel spinning tool. *The International Journal of Advanced Manufacturing Technology*, 2017. 92.

[4] HOU, Y., et al. A Review of Characterization and Modelling Approaches for Sheet Metal Forming of Lightweight Metallic Materials. *Materials*, 2023. 16, DOI: 10.3390/ma16020836.

[5] MIKLÓS, T., Development of Lightweight Steels for Automotive Applications, in Engineering Steels and High Entropy-Alloys, S. Ashutosh, D. Zoia, and K. Sanjeev, Editors. 2020, IntechOpen: Rijeka. p. Ch. 6.

[6] ABD-ELTWAB, A.A., et al., An Investigation into the Forming of Tube Ends Using the Ballizing Process. *Design Engineering (Toronto)* 2022. I: p. 3358 - 3374.

[7] QUIGLEY, E. AND J. MONAGHAN, Metal forming: an analysis of spinning processes. *Journal of Materials Processing Technology*, 2000. 103(1): p. 114-119.

[8] MATUKHNO, N., et al., Cyclic bending under tension of alloy AZ31 sheets: Influence on elongation-to-fracture and strength. *Materials Science and Engineering*: A, 2022. 857: p. 144127.

[9] GONDO, S., et al., Evolution of texture distribution in thickness direction of aluminum sheet in metal spinning. *Materials Characterization*, 2022. 188: p. 111877.

[10] GAO, P.F., et al., Deformation mode and wall thickness variation in conventional spinning of metal sheets. *International Journal of Machine Tools and Manufacture*, 2022. 173: p. 103846.

[11] RIAZ, A.A., et al., Experimental investigations on the effects of rotational speed on temperature and microstructure variations in incremental forming of T6-tempered and annealed AA2219 aerospace alloy. *Metals*, 2020. 10(6): p. 1-18.

[12] LI, Z., et al. Roller trace design in multi-pass conventional spinning based on cylindrical part. in ASME International Mechanical Engineering Congress and Exposition, *Proceedings (IMECE)*. 2020.

[13] BÍLEK, O., Et Al., Mathematical Methods of Surface Roughness Evaluation of Areas with A Distinctive Inclination. *Manufacturing Technlogy* 2018. 18(3): P. 363-368.

[14] KOREČEK, D., P. SOLFRONK, AND J.J.M.T.J. SOBOTKA, Numerical Simulation as A Tool to Predict Sheet Metal Forming Process of TRIP Steel HCT690. *Manufacturing Technology* 2020. 20(5): P. 625-631.

[15] GIULIANO, G., Et Al., Cold Blow Forming of a Thin Sheet in AA8006 Aluminum Alloy. *Manufacturing Technology* 2023. 23(3): P. 284-289.

[16] SUI, L., Et Al., Finite Element Simulation of Cylinder Closure Spinning. *Manufacturing Technology* 2023. 23(3): P. 333-340.

[17] ATIA, K.M., Et Al., An Investigation into A Conventional Spinning Process Combined with Flow Forming with Simultaneously Burnishing Processes. *Journal Of Advanced Engineering Trends*, 2021. 40(1): P. 97-107.

[18] ATIA, K., ET AL., A Novel Technique for Combining Conventional and Flow Spinning with Simultaneously Burnishing Processes. 2020.